

Phase separation of atomic Bose-Fermi mixtures in an optical lattice

H.P. Büchler and G. Blatter

Theoretische Physik, ETH-Hönggerberg, CH-8093 Zürich, Switzerland

(Dated: February 2, 2008)

We study a two-dimensional atomic mixture of bosons and fermions cooled into their quantum degenerate states and subject to an optical lattice. The optical lattice provides van Hove singularities in the fermionic density of states. We find that these van Hove singularities produce new and interesting features for the transition towards phase separation: an arbitrary weak interaction between the bosons and the fermions is sufficient to drive the phase separation at low temperatures. The phase separated state turns stable for attractive and repulsive interaction between the bosons and fermions and can be cast into the standard form of a ‘liquid–gas’ transition.

I. INTRODUCTION

Atomic mixtures of bosons and fermions represent a new laboratory system for the study of quantum degenerate matter. A major experimental breakthrough is the sympathetic cooling of atomic fermions into their quantum degenerate state [1, 2, 3, 4] allowing for the realization of new thermodynamic phase transitions. The main focus is on the superfluid transition of atomic fermions [5, 6, 7, 8], and the appearance of complex quantum phases in the presence of an optical lattice, such as supersolids [9] and nontrivial Mott insulating phases [10]. In addition, a Bose-Fermi mixture cooled into its quantum degenerate state shows a strong tendency towards phase separation and the demixing of the bosons and fermions [11, 12]. While this phase separation itself exhibits many fascinating phenomena [13, 14, 15, 16], it also represents a major drawback of Bose-Fermi mixtures as it restricts the allowed parameter range for the observation of complex quantum phases, see e.g., the competition between phase separation and a supersolid phase as discussed in Ref. 9. The analysis of phase separation in Bose-Fermi mixtures then contributes to our basic understanding of atomic gases as needed in future studies of other novel quantum phases.

The main mechanism driving the phase separation is a small perturbation of the bosonic density δn_B inducing a modulation of the fermionic density $\delta n_F \sim -U_{FB}N(\epsilon_F)\delta n_B$. Here, $N(\epsilon_F)$ denotes the density of states at the Fermi energy ϵ_F and U_{FB} is the strength of the interaction between the bosons and the fermions. This fermionic distortion acts back onto the bosons and produces a shift of the bosonic energy $-U_{FB}^2N(\epsilon_F)\delta n_B^2/2$, thereby inducing an attraction between the bosons with strength $U_{FB}^2N(\epsilon_F)$. Phase separation appears if the induced attraction is of the same order as the intrinsic repulsion U_B between the bosons.

Previous work on phase separation in Bose-Fermi mixtures concentrated on the $T = 0$ limit. The phase separation is triggered by changing the interaction U_{FB} and results in minimal energy configurations involving separated states with two pure phases, two differently mixed phases, or one pure phase coexisting with one mixed phase. Assuming a repulsive interaction between the

fermions and the bosons, the phase separation of Bose-Fermi mixtures in a 3D harmonic trap results in an increased bosonic density accumulated in the center of the trap and surrounded by a fermionic shell [11, 12, 13]. A thermodynamic analysis of the homogeneous situation [15] has shown that the criterion for phase separation described above is preempted by a first-order scenario resulting in a separation involving a mixed and a pure phase. On the other hand, an attractive interaction between the bosons and fermions triggers a system collapse above a critical boson number [16]; such a collapse has been recently observed in an experiment by Modugno *et al.* [14].

Here, we concentrate on the behavior of phase separation in a situation, where the fermionic density of states is strongly modified by the presence of an optical lattice. Of special interest is the two-dimensional (2D) situation where the presence of saddle points in the fermionic dispersion relation $\epsilon_F(\mathbf{k})$ provides logarithmic van Hove singularities in the density of states $N(\epsilon) \sim N_0 \ln |2W_F/(\epsilon - \epsilon_0)|$, with W_F the band width and ϵ_0 the position of the van Hove singularity. A finite temperature T cuts this singularity and the system response becomes strongly temperature dependent, resulting in a smooth transition with decreasing temperature into a phase-separated state with two mixed phases. Below, we present a detailed analysis of this finite temperature phase transition. We find that the van Hove singularities strongly enhance the tendency towards phase separation, with an arbitrary weak interaction between the bosons and the fermions already sufficient to drive the transition at low temperatures. The transition is of the ‘liquid–gas’ transition type and the phase separated state is stable for attractive as well as for repulsive interaction between the bosons and fermions. Concentrating on the weak coupling limit, we derive the n_F - T phase diagram involving two mixed Bose-Fermi gases with slightly different fermion density δn_F . Here, we focus on phase separation and ignore other possible instabilities in the system, e.g., BCS-superconductivity or supersolid formation. Note that these competing phases also exhibit a strong increase of the critical temperature due to the van Hove singularity, a phenomenon well studied in BCS-superconductivity [17]. Furthermore, our weak coupling analysis with $U_{FB}^2N_0 \ll U_B$ excludes the appearance of

a competing first-order phase transition of the type discussed in Ref. 15.

The Hamiltonian of an interacting Bose-Fermi mixture subject to an optical lattice is presented in Sec. II. We make use of the tight-binding approximation to cast the Hamiltonian in a form describing a Bose-Fermi mixture on a lattice. We then integrate out the fermions and arrive at an effective boson Hamiltonian. The interaction becomes strongly temperature dependent and the effective boson Hamiltonian exhibits an instability towards phase separation at a critical temperature T_{PS} . This instability is further examined in Sec. III and the phase separated state is studied within the Thomas-Fermi description; the results are summarized in a phase diagram exhibiting all the properties of a standard liquid-gas transition. Finally, we study the impact of this transition on an atomic Bose-Fermi mixture in a finite trap in Sec. IV.

II. BOSE-FERMI MIXTURES

We start with interacting bosons and fermions in two dimensions. Such a 2D setup is achieved via application of a strong confining potential in the transverse direction. The Hamiltonian for interacting bosons and fermions subject to an optical lattice takes the form $H = H_{\text{B}} + H_{\text{F}} + H_{\text{int}}$ with

$$\begin{aligned} H_{\text{B}} &= \int d\mathbf{x} \, \psi_{\text{B}}^+ \left(-\frac{\hbar^2}{2m_{\text{B}}} \Delta + V_{\text{B}}(\mathbf{x}) \right) \psi_{\text{B}}, \\ H_{\text{F}} &= \int d\mathbf{x} \, \psi_{\text{F}}^+ \left(-\frac{\hbar^2}{2m_{\text{F}}} \Delta + V_{\text{F}}(\mathbf{x}) \right) \psi_{\text{F}}, \\ H_{\text{int}} &= \int d\mathbf{x} \left(g_{\text{FB}} \psi_{\text{B}}^+ \psi_{\text{B}} \psi_{\text{F}}^+ \psi_{\text{F}} + \frac{1}{2} g_{\text{B}} \psi_{\text{B}}^+ \psi_{\text{B}}^+ \psi_{\text{B}} \psi_{\text{B}} \right). \end{aligned} \quad (1)$$

Here, ψ_{F} and ψ_{B} denote the fermionic and bosonic field operators, while the interaction between the particles is taken into account within the pseudopotential approximation. We assume a repulsive interaction $g_{\text{B}} = 4\pi a_{\text{B}} \hbar^2 / m_{\text{B}}$ between the bosons with the scattering length $a_{\text{B}} > 0$, while the coupling $g_{\text{FB}} = 2\pi a_{\text{FB}} \hbar^2 / \mu$ accounts for the interaction between the fermions and the bosons with μ the relative mass and a_{FB} the boson-fermion scattering length of either sign. Furthermore, we restrict the analysis to spinless fermions; such a spinless fermionic atomic gas is naturally achieved in an experiment via spin polarization. Then, the s -wave scattering length of the fermion-fermion interaction vanishes, while p -wave scattering is suppressed at low energies and is neglected in the following analysis. The optical lattice with wave length λ provides an $a = \lambda/2$ -periodic potential for the bosons ($\alpha = \text{B}$) and fermions ($\alpha = \text{F}$) with $V_{\alpha}(\mathbf{x}) = V_{\alpha} \sin^2(\pi x/a) + V_{\alpha} \sin^2(\pi y/a) + V_{\alpha}^t$, while the trapping potential V_{α}^t accounts for the strong transverse confining $m_{\alpha} \omega_{\alpha\perp}^2 z^2 / 2$ establishing a two dimensional setup, and for the weak longitudinal trapping $m_{\alpha} \omega_{\alpha\parallel}^2 (x^2 + y^2) / 2$.

A. Hamiltonian within tight-binding approximation

In the following, we focus on strong optical lattices $V_{\alpha} > E_{\alpha} = 2\hbar^2 \pi^2 / \lambda^2 m_{\alpha}$ and weak interactions. Then, in analogy to the mapping onto the Bose-Hubbard model [18], we transform the Hamiltonian (1) for the Bose-Fermi mixture to a simplified Hamiltonian of the tight-binding form. We restrict the analysis to the lowest Bloch band and introduce the Bloch wave functions $v_{\mathbf{k}}$ (fermions) and $w_{\mathbf{k}}$ (bosons) of the corresponding single particle problem in the 2D periodic potential. In turn, the Bloch wave functions $w_{\mathbf{k}}(\mathbf{x})$ and $v_{\mathbf{k}}(\mathbf{x})$ are related to the Wannier functions $\tilde{w}(\mathbf{x} - \mathbf{R})$ and $\tilde{v}(\mathbf{x} - \mathbf{R})$ according to

$$\tilde{w}(\mathbf{x} - \mathbf{R}) = \frac{1}{N} \sum_{\mathbf{k} \in K} w_{\mathbf{k}}(\mathbf{x}) \exp(-i\mathbf{R}\mathbf{k}), \quad (2)$$

$$\tilde{v}(\mathbf{x} - \mathbf{R}) = \frac{1}{N} \sum_{\mathbf{k} \in K} v_{\mathbf{k}}(\mathbf{x}) \exp(-i\mathbf{R}\mathbf{k}), \quad (3)$$

with \mathbf{R} a lattice vector and K the first Brillouin zone of the reciprocal lattice. Here, we have introduced the quantization volume $V = Na^2$ with N the number of unit cells. In the following, $n_{\text{F,B}}$ denote the number of particles per unit cell. We express the bosonic and fermionic field operators $\psi_{\text{F,B}}$ in terms of the Bloch wave functions $w_{\mathbf{k}}$ and $v_{\mathbf{k}}$, or equivalently, in terms of the Wannier functions \tilde{w} and \tilde{v}

$$\psi_{\text{B}}^+(\mathbf{x}) = \frac{1}{\sqrt{N}} \sum_{\mathbf{k} \in K} w_{\mathbf{k}}(\mathbf{x}) b_{\mathbf{k}}^+ = \sum_{\mathbf{R}} \tilde{w}(\mathbf{x} - \mathbf{R}) b_{\mathbf{R}}^+, \quad (4)$$

$$\psi_{\text{F}}^+(\mathbf{x}) = \frac{1}{\sqrt{N}} \sum_{\mathbf{k} \in K} v_{\mathbf{k}}(\mathbf{x}) c_{\mathbf{k}}^+ = \sum_{\mathbf{R}} \tilde{v}(\mathbf{x} - \mathbf{R}) c_{\mathbf{R}}^+. \quad (5)$$

The bosonic creation operator $b_{\mathbf{k}}^+$ of the Bloch wave state $w_{\mathbf{k}}$ is the Fourier transform of the bosonic creation operator $b_{\mathbf{R}}^+$ for the Wannier state $\tilde{w}(\mathbf{x} - \mathbf{R})$ with

$$b_{\mathbf{R}}^+ = \frac{1}{\sqrt{N}} \sum_{\mathbf{k} \in K} \exp(i\mathbf{k}\mathbf{R}) b_{\mathbf{k}}^+, \quad (6)$$

and analogously for the fermionic creation operators $c_{\mathbf{k}}^+$ and $c_{\mathbf{R}}^+$. In our subsequent analysis it is convenient to use the operators $b_{\mathbf{k}}^+$ and $c_{\mathbf{k}}^+$. Inserting the expansion (5) into the Hamiltonian (1) and restricting the analysis to on-site interactions, the Hamiltonian of the Bose-Fermi mixture (1) reduces to

$$\begin{aligned} H &= \sum_{\mathbf{k} \in K} \epsilon_{\text{B}}(\mathbf{k}) b_{\mathbf{k}}^+ b_{\mathbf{k}} + \frac{U_{\text{B}}}{2N} \sum_{\{\mathbf{k}, \mathbf{k}', \mathbf{q}, \mathbf{q}'\}} b_{\mathbf{k}}^+ b_{\mathbf{q}}^+ b_{\mathbf{k}'} b_{\mathbf{q}'} \\ &+ \sum_{\mathbf{q} \in K} \epsilon_{\text{F}}(\mathbf{q}) c_{\mathbf{q}}^+ c_{\mathbf{q}} + \frac{U_{\text{FB}}}{N} \sum_{\{\mathbf{k}, \mathbf{k}', \mathbf{q}, \mathbf{q}'\}} b_{\mathbf{k}}^+ b_{\mathbf{k}'} c_{\mathbf{q}}^+ c_{\mathbf{q}'}. \end{aligned} \quad (7)$$

The summation $\{\mathbf{k}, \mathbf{k}', \mathbf{q}, \mathbf{q}'\}$ is restricted to $\mathbf{k}, \mathbf{k}', \mathbf{q}, \mathbf{q}' \in K$ and the momentum conservation $\mathbf{k} - \mathbf{k}' + \mathbf{q} - \mathbf{q}' = \mathbf{K}_m$

with \mathbf{K}_m a reciprocal lattice vector; a scattering event involving such a vector \mathbf{K}_m is an Umklapp process. The interaction parameters involve the Wannier functions \tilde{w} and \tilde{v} and take the form

$$U_B = g_B \int d\mathbf{x} |\tilde{w}(\mathbf{x})|^4, \quad (8)$$

$$U_{FB} = g_{FB} \int d\mathbf{x} |\tilde{w}(\mathbf{x})|^2 |\tilde{v}(\mathbf{x})|^2, \quad (9)$$

while $\epsilon_F(\mathbf{k})$ and $\epsilon_B(\mathbf{k})$ denote the lowest energy bands for the fermions and bosons, respectively.

In a two dimensional system, the band structure $\epsilon_F(\mathbf{k})$ exhibits saddle points at wave vectors \mathbf{k}_{0i} and energies $\epsilon_{0i} = \epsilon_F(\mathbf{k}_{0i})$. Lattice symmetries naturally produce several saddle points at the same energy ϵ_0 ; we denote their number by z . Close to such a saddle point, the dispersion relation $\epsilon_F(\mathbf{k})$ is quadratic, and can be expanded along the principal axes ($\mathbf{k} = \mathbf{k}_0 + \mathbf{k}_\perp + \mathbf{k}_\parallel$)

$$\epsilon_F(\mathbf{k}) \sim \epsilon_0 + \frac{\hbar^2}{2m_\perp} \mathbf{k}_\perp^2 - \frac{\hbar^2}{2m_\parallel} \mathbf{k}_\parallel^2. \quad (10)$$

The saddle point gives rise to van Hove singularities in the density of states (per site) for $\epsilon \rightarrow \epsilon_0$,

$$N(\epsilon) \sim N_0 \ln \left| \frac{2W_F}{\epsilon - \epsilon_0} \right| \quad (11)$$

with the band width W_F , and the prefactor $N_0 = z(m_\perp m_\parallel)^{1/2} (a^2/2\pi^2 \hbar^2)$. This logarithmic singularity plays a crucial role in the study of phase separation in Bose-Fermi mixtures and will be examined in detail in the following. Note, that the situation is different in 3D systems, where the density of states is regular, and singularities appear only in quantities involving derivatives of the density of states.

As an example we study the dispersion relation for a strong optical lattice with only nearest neighbor hopping,

$$\epsilon_F(\mathbf{q}) = -2J_F \left[\cos\left(q_x \frac{\lambda}{2}\right) + \cos\left(q_y \frac{\lambda}{2}\right) \right] \quad (12)$$

and J_F the hopping energy. The density of states is irregular and exhibits a logarithmic van Hove singularity at $\epsilon_0 = 0$ arising from saddle points at $\mathbf{k}_0 = (\pi/a, 0)$ and $\mathbf{k}_0 = (0, \pi/a)$,

$$N(\epsilon) = N_0 K \left[\sqrt{1 - \frac{\epsilon^2}{16J_F^2}} \right] \sim N_0 \ln \left| \frac{16J_F}{\epsilon} \right|, \quad (13)$$

with $N_0 = 1/(2\pi^2 J_F)$, and $K[m]$ the complete elliptic integral of the first kind [19]. The hopping amplitude J_F derives from the exactly known width of the lowest band in the 1D Mathieu equation [20]

$$4J_F = \frac{16}{\sqrt{\pi}} \sqrt{E_F V_F} \left(\frac{V_F}{E_F} \right)^{1/4} \exp \left(-2\sqrt{\frac{V_F}{E_F}} \right). \quad (14)$$

A reliable estimate of the interaction strength is provided by approximating the Wannier functions $\tilde{w}(\mathbf{x})$ and $\tilde{v}(\mathbf{x})$ by the wave function of the harmonic oscillator in each well. The oscillator frequency in each well is given by $\omega_{\text{well}} = \sqrt{4E_\alpha V_\alpha}/\hbar$ with $\alpha = B, F$, which implies a size $a_{\text{well}} = \sqrt{\hbar/m\omega_{\text{well}}}$ for the localized wave function. The interaction strengths U_{FB} and U_B , cf. (8) and (9), assume the form

$$U_B = 8\sqrt{\pi} E_B \frac{a_B}{\lambda} \left(\frac{\hbar\omega_{F\perp}}{2E_B} \right)^{1/2} \left(\frac{V_B}{E_B} \right)^{1/2}, \quad (15)$$

$$U_{FB} = 8\sqrt{\pi} \sqrt{E_B E_F} \frac{a_{FB}}{\lambda} \left(\frac{\hbar\omega_{F\perp}}{2E_F} \frac{\hbar\omega_{B\perp}}{2E_B} \right)^{1/4} \left(\frac{V_F}{E_F} \frac{V_B}{E_B} \right)^{1/4}.$$

The validity of the derivation of the Hamiltonian (7) requires that the interaction parameters U_B and U_{FB} are small compared to the energy gap $\sim \hbar\omega_{\text{well}}$ separating the lowest Bloch band from the next higher.

B. Effective boson Hamiltonian

In order to study the stability of the ground state, it is convenient to derive an effective Hamiltonian for the bosons alone. This effective Hamiltonian accounts for the fermions via a modified interaction between the bosons. We start with linear response theory, where the boson density $n_B(\mathbf{q})$ drives the fermionic system $\langle n_F(\mathbf{q}) \rangle = U_{FB} \chi(T, \mathbf{q}) n_B(\mathbf{q})$ with $\chi(T, \mathbf{q})$ the response function of the fermions at temperature T . This perturbed fermionic density in turn acts as a drive for the bosons and is accounted for by the effective interaction between the bosons

$$H_{\text{int}} = \frac{1}{2N} \sum_{\{\mathbf{k}, \mathbf{k}', \mathbf{q}, \mathbf{q}'\}} [U_B + U_{FB}^2 \chi(T, \mathbf{q} - \mathbf{q}')] b_{\mathbf{k}}^+ b_{\mathbf{k}'} b_{\mathbf{q}}^+ b_{\mathbf{q}'}. \quad (16)$$

The response function of the fermions is given by the Lindhard function

$$\chi(T, \mathbf{q}) = \int_K \frac{d\mathbf{k}}{v_0} \frac{f[\epsilon_F(\mathbf{k})] - f[\epsilon_F(\mathbf{k} + \mathbf{q})]}{\epsilon_F(\mathbf{k}) - \epsilon_F(\mathbf{k} + \mathbf{q}) + i\eta} \quad (17)$$

with $v_0 = (2\pi/a)^2$ the volume of the first Brillouin zone. The temperature T enters via the Fermi distribution function $f(\epsilon) = 1/\{1 + \exp[(\epsilon - \mu_F)/T]\}$. We focus on static instabilities of the ground state and neglect the frequency dependence of the response function. A rigorous derivation of the effective action including its time dependence can be achieved within a path integral approach [21].

III. PHASE SEPARATION

A. Instability at $q = 0$

The Lindhard function is always negative and induces an attraction between the bosons independent of the at-

tractive/repulsive nature of the original coupling U_{FB} between the bosons and fermions. The effective long distance scattering parameter for $\mathbf{q} \rightarrow 0$ takes the form

$$U_{\text{eff}} = U_{\text{B}} + U_{\text{FB}}^2 \chi(T, 0). \quad (18)$$

For a fermionic system with a regular density of states, the Lindhard function at $\mathbf{q} = 0$ and low temperatures reduces to $\chi(T \rightarrow 0, 0) = -N(\epsilon_{\text{F}})$ with $N(\epsilon)$ the fermionic density of states and ϵ_{F} the Fermi energy. For fermions on a square lattice in 2D the density of states is irregular and exhibits a logarithmic van Hove singularity at ϵ_0 , see Eq. (13). For a fermionic filling such that the Fermi energy ϵ_{F} matches the energy of the van Hove singularity, i.e. $\epsilon_{\text{F}} = \epsilon_0$, the Lindhard function diverges logarithmically for $T \rightarrow 0$, and its asymptotic behavior takes the form

$$\chi(T \rightarrow 0, 0) = \int d\epsilon N(\epsilon) \frac{\partial f(\epsilon)}{\partial \epsilon} = -N_0 \ln \frac{2c_1 W_{\text{F}}}{T} \quad (19)$$

with $c_1 = 2 \exp(C)/\pi \approx 1.13$ a numerical prefactor and $C \approx 0.577$ the Euler constant.

As a consequence of this logarithmic divergence of the Lindhard function for $T \rightarrow 0$, the effective scattering parameter U_{eff} always turns negative at low temperatures. Since a thermodynamically stable superfluid condensate requires a positive effective interaction $U_{\text{eff}} > 0$ [22], the system exhibits an instability at the critical temperature T_{PS} defined via $U_{\text{eff}}(T_{\text{PS}}) = 0$. Using Eqs. (18) and (19), we find the critical temperature

$$T_{\text{PS}} = 2c_1 W_{\text{F}} \exp[-1/\lambda_{\text{FB}}] \quad (20)$$

with $\lambda_{\text{FB}} = (U_{\text{FB}}^2/U_{\text{B}})N_0$ the dimensionless coupling constant. Note, that weak coupling requires $\lambda_{\text{FB}} < 1$ and the critical temperature T_{PS} is well below the transition temperature T_{KT} of the superfluid condensate. Below the critical temperature T_{PS} the effective interaction U_{eff} turns negative providing a negative compressibility, and the homogeneous superfluid condensate becomes unstable. Then, the new ground state with fixed averaged density n_{B} and n_{F} exhibits phase separation with areas of increased and decreased local densities coexisting.

Note, that this transition towards phase separation exhibits two major differences as compared to the phase separation discussed in Refs. [11, 15]. First, the phase separation is an instability appearing at low temperatures for arbitrary small coupling U_{FB} between the bosons and fermions. Second, the increase/decrease in the bosonic density drives the fermionic density away from a filling factor close to the van Hove singularity providing a regular $\chi(T, 0)$ which in turn stabilizes the system.

B. Thomas-Fermi approximation

In the following, we study the phase separated state within the Thomas-Fermi theory. Within this theory, we introduce two densities $n_{\text{B}}(\mathbf{x})$ and $n_{\text{F}}(\mathbf{x})$ which are

smooth on a scale large compared to the Fermi wave length $1/k_{\text{F}}$ and the bosonic coherence length $\xi = 1/(8\pi n a_{\text{B}})^{1/2}$. Then, the system is in thermodynamic equilibrium at every position and neglecting the kinetic energy of the bosons the free energy $\mathcal{F}[n_{\text{B}}, n_{\text{F}}]$ of the system becomes

$$\mathcal{F}[n_{\text{B}}, n_{\text{F}}] = \int \frac{d\mathbf{x}}{a^2} \left\{ F_{\text{F}}[n_{\text{F}}(\mathbf{x})] + V_{\text{F}}^t(\mathbf{x})n_{\text{F}}(\mathbf{x}) + V_{\text{B}}^t(\mathbf{x})n_{\text{B}}(\mathbf{x}) + \frac{1}{2}U_{\text{B}}n_{\text{B}}(\mathbf{x})n_{\text{B}}(\mathbf{x}) + U_{\text{FB}}n_{\text{B}}(\mathbf{x})n_{\text{F}}(\mathbf{x}) \right\}. \quad (21)$$

Here, we include the weak external trapping potential V_{B}^t for the bosons and V_{F}^t for the fermions. Furthermore, the appearance of the instability requires that the critical temperature T_{PS} is large compared to the mean level spacing introduced by the external trapping potentials, i.e., $T_{\text{PS}} \gg \hbar\omega$ with ω a characteristic trapping frequency. Note, that we assume $T \ll T_{\text{KT}}$ which implies that the influence of thermally excited bosons is small and can be neglected. The local free energy $F_{\text{F}}[n_{\text{F}}]$ of the fermions at temperature T takes the form ($F = \Omega - \mu n$)

$$F_{\text{F}}[n_{\text{F}}] = -T \int d\epsilon N(\epsilon) \ln \left[1 + \exp \left(-\frac{\epsilon - \mu}{T} \right) \right] - \mu n_{\text{F}}. \quad (22)$$

The local chemical potential $\mu(\mathbf{x})$ is determined by the condition that the fermionic free energy F_{F} is a minimum, i.e., $\partial_{\mu} F_{\text{F}} = 0$, and hence

$$n_{\text{F}}(\mathbf{x}) = \int d\epsilon N(\epsilon) f[\epsilon - \mu(\mathbf{x})]. \quad (23)$$

Furthermore, the total number of particles in the system is fixed providing the additional constraints

$$N_{\text{F}} = \int d\mathbf{x} n_{\text{F}}(\mathbf{x}), \quad N_{\text{B}} = \int d\mathbf{x} n_{\text{B}}(\mathbf{x}). \quad (24)$$

The ground state configuration at temperature T is determined by the minima of the functional $\mathcal{F}[n_{\text{B}}, n_{\text{F}}]$ satisfying the conditions (24), and hence

$$\mu[n_{\text{F}}(\mathbf{x})] + V_{\text{F}}^t(\mathbf{x}) + U_{\text{FB}}n_{\text{B}}(\mathbf{x}) = \mu_{\text{F}}, \quad (25)$$

$$U_{\text{B}}n_{\text{B}}(\mathbf{x}) + V_{\text{B}}^t(\mathbf{x}) + U_{\text{FB}}n_{\text{F}}(\mathbf{x}) = \mu_{\text{B}}, \quad (26)$$

with μ_{F} and μ_{B} the Laplace multipliers introduced to account for (24). These parameters act as global chemical potentials for the system (we have used the relation $\partial_{n_{\text{F}}} F_{\text{F}}[n_{\text{F}}] = \mu[n_{\text{F}}]$).

In the following, we neglect the trapping potentials V_{F}^t and V_{B}^t and analyze the stability of the state with a homogeneous fermionic and bosonic density n_{F} and n_{B} . Then, Eqs. (25) and (26) can be cast into a simpler form. From Eq. (26), we obtain the bosonic density $n_{\text{B}} = (\mu_{\text{B}} - U_{\text{FB}}n_{\text{F}})/U_{\text{B}}$ and inserting this result into Eq. (25), we obtain

$$\mu[n_{\text{F}}] = \mu_{\text{F}} - \frac{U_{\text{FB}}}{U_{\text{B}}} \mu_{\text{B}} + \frac{U_{\text{FB}}^2}{U_{\text{B}}} n_{\text{F}}. \quad (27)$$

Using (23) we arrive at an implicit equation for n_F at fixed global chemical potentials μ_F and μ_B ,

$$n_F = \int d\epsilon N(\epsilon) f \left(\epsilon - \mu_F + \frac{U_{FB}}{U_B} \mu_B - \frac{U_{FB}^2}{U_B} n_F \right). \quad (28)$$

A solution of (28) with fermionic and bosonic densities n_F and n_B is a local minimum of the functional (21), if the Hessian

$$\mathbf{H} = \begin{pmatrix} \partial_{n_F} \mu[n_F] & U_{FB} \\ U_{FB} & U_B \end{pmatrix} \quad (29)$$

is positive definite. The derivative $\partial_{n_F} \mu[n_F]$ is related to the response function $\chi(T, \mathbf{q})$ via the compressibility sum rule and takes the form

$$\partial_{n_F} \mu[n_F] = \left\{ \int d\epsilon N(\epsilon) [-\partial_\epsilon f(\epsilon - \mu)] \right\}^{-1} \quad (30)$$

$$= -[\chi(T, 0)]^{-1}. \quad (31)$$

A positive definite Hessian imposes the stability conditions

$$\text{Tr} \mathbf{H} = |\chi(T, 0)| + U_B > 0, \quad (32)$$

$$\det \mathbf{H} = |\chi(T, 0)|^{-1} U_B - U_{FB}^2 > 0. \quad (33)$$

The first condition is always satisfied for a repulsive interaction $U_B > 0$ between the bosons. For a regular density of states $N(\epsilon)$, the second stability condition at zero temperature $T = 0$ becomes

$$\frac{U_{FB}^2}{U_B} N(\epsilon_F) = 1 \quad (34)$$

and coincides with the condition for phase separation in Refs. 11, 15; ϵ_F denotes the Fermi energy.

However, for the system considered here with 2D fermions on a square lattice the density of states exhibits a van Hove singularity. A setup with a fermionic density \bar{n}_F matching the van Hove singularity at ϵ_0 and arbitrary bosonic density \bar{n}_B then is of special interest. These densities have to satisfy the conditions (25) and (26), from which we find the appropriate global chemical potentials $\bar{\mu}_B = U_{FB} \bar{n}_F + U_B \bar{n}_B$ and, using $\mu[\bar{n}_F] = \epsilon_0$, $\bar{\mu}_F = U_{FB} \bar{n}_B + \epsilon_0$. Fixing the global chemical potentials $\bar{\mu}_F$ and $\bar{\mu}_B$ rather than the densities \bar{n}_F and \bar{n}_B , we can allow for the appearance of new solutions, i.e., phase separation. The new fermion density n_F then has to satisfy the condition (28) at fixed values $\bar{\mu}_B$ and $\bar{\mu}_F$ of the chemical potentials,

$$n_F = \int d\epsilon N(\epsilon) f \left(\epsilon - \epsilon_0 - \frac{U_{FB}}{U_B} (n_F - \bar{n}_F) \right). \quad (35)$$

The self-consistency equation (35) has the obvious solution $n_F = \bar{n}_F$. This solution turns unstable at the point where the second stability condition (33) is violated: defining the deviation $\delta \bar{n}_F = n_F - \bar{n}_F$ and expanding (35) around \bar{n}_F we find that

$$\alpha(T) \delta \bar{n}_F + \beta(T) (\delta \bar{n}_F)^2 + \gamma(T) (\delta \bar{n}_F)^3 = 0, \quad (36)$$

where $\alpha(T) = [1 + (U_{FB}^2/U_B) \int d\epsilon N(\epsilon + \epsilon_0) \partial_\epsilon f(\epsilon)] \approx \alpha_0(T - T_{PS})$, while $\beta(T)$ and $\gamma(T) > 0$ depend only weakly on temperature. For a system with particle-hole symmetry the quadratic term vanishes, i.e., $\beta(T) = 0$; this is the case for the situation discussed above with the dispersion relation (12) and a half-filled band with Fermi energy $\epsilon_F = 0$. The sign change in $\alpha(T)$ at T_{PS} matches up with the violation of (33) and the expression for the transition temperature T_{PS} agrees with the one derived previously in (20). At high temperatures $T > T_{PS}$, $\alpha > 0$ and Eq. (35) has only the trivial solution $\bar{n}_F = 0$. For low temperatures $T < T_{PS}$, $\alpha < 0$ and two new solutions $\bar{n}_F \pm \delta \bar{n}_F$ appear with

$$\delta \bar{n}_F = \sqrt{\alpha_0/\gamma} (T_{PS} - T)^{1/2}, \quad (37)$$

where we assume $\beta = 0$ and T close to T_{PS} .

At zero temperature and for $\lambda_{FB} \ll 1$ we find the density change

$$\begin{aligned} \delta \bar{n}_F &= \frac{U_{FB}^2}{U_B} \int_0^{\delta n_F} dn N \left(\epsilon_0 + \frac{U_{FB}}{U_B} n \right) \\ &\sim \delta \bar{n}_F \lambda_{FB} \ln \left(\frac{16c_2 J_F U_B}{U_{FB}^2 |\delta \bar{n}_F|} \right) \end{aligned} \quad (38)$$

with $c_2 = \exp(1)$. Solving for $\delta \bar{n}_F$ provides us with the following shifts in the fermionic and bosonic densities

$$\begin{aligned} n_F - \bar{n}_F &= \delta \bar{n}_F = \pm 16c_2 \frac{U_B J_F}{U_{FB}^2} \exp \left(-\frac{1}{\lambda_{FB}} \right), \\ n_B - \bar{n}_B &= -\frac{U_{FB}}{U_B} \delta \bar{n}_F = \mp 16c_2 \frac{J_F}{U_{FB}} \exp \left(-\frac{1}{\lambda_{FB}} \right). \end{aligned} \quad (39)$$

The relation between the $T = 0$ density shift $\delta \bar{n}_F$ and the critical temperature T_{PS} takes the form

$$\frac{U_{FB}^2}{U_B} \frac{\delta \bar{n}_F}{T_{PS}} = c_2/c_1 \approx 2.40. \quad (40)$$

Inserting the solutions (39) into the free energy (21) provides us with the energy shift per unit cell at zero temperature

$$\frac{\Delta \mathcal{F}}{N} = -\frac{U_{FB}^2}{2U_B} (\delta \bar{n}_F)^2. \quad (41)$$

C. Phase diagram

The solution discussed above allows us to find the phase diagram of the system. At low temperature $T < T_{PS}$, we distinguish between a low-density ‘gas’ phase with $n_F \leq \bar{n}_F - \delta \bar{n}_F$, and a high-density ‘fluid’ phase with $n_F \geq \bar{n}_F + \delta \bar{n}_F$. The bosonic density derives from $n_B = (\mu_B - U_{FB} n_F)/U_B$. For a repulsive interaction $U_{FB} > 0$ the fermionic low-density phase partners up with a high bosonic density, while for attractive interaction $U_{FB} < 0$ the fermionic low-density phase implies a low bosonic density.

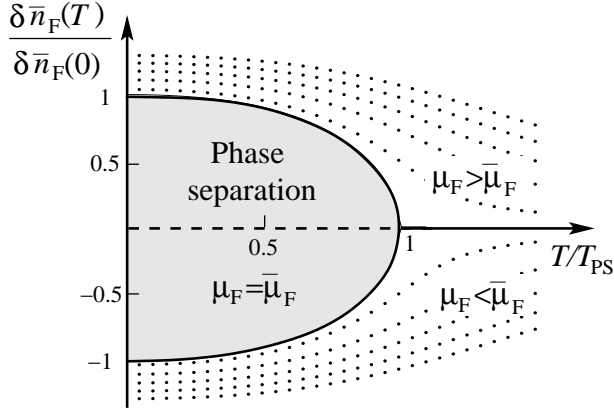


FIG. 1: n_F - T phase diagram. The grey region denotes the phase separated regime, while the solid line denotes the line of fixed chemical potential $\bar{\mu}_F$. The dotted lines describe fixed chemical potentials $(\mu_F - \bar{\mu}_F)/T_{PS} = \pm 0.02, 0.06, 0.01, 0.14, 0.18$. The lines derive from Eq. (28) with $\lambda = 0.2$ and the dispersion relation (12).

The phase transition is of the standard liquid-gas transition type, see Fig. 1. At temperatures below critical, $T < T_{PS}$, the low-density ‘gas’ phase is separated by a first-order phase transition from the high-density ‘liquid’ phase. The transition is driven by the chemical potential and takes place at the critical value

$$\bar{\mu}_F = \frac{U_{FB}}{U_B} \bar{\mu}_B - \frac{U_{FB}^2}{2U_B}, \quad (42)$$

cf. Eq. (27), where we have used the results $\epsilon_0 = 0$ and $\bar{n}_F = 1/2$ valid for the dispersion (12). A fixed averaged fermionic density between $\bar{n}_F - \delta\bar{n}_F < n_F < \bar{n}_F + \delta\bar{n}_F$ is only realized via coexistence of the low density ‘gas’ phase and the high density ‘liquid’ phase. The first order transition terminates in a critical endpoint at the temperature T_{PS} and density $n_F = \bar{n}_F$. Varying the temperature across the critical value T_{PS} along the isochore $n_F = \bar{n}_F$, we obtain a second-order phase transition between the homogeneous phase and the phase separated state, see Fig. 1. This transition appears for arbitrary weak coupling U_{FB} due to the enhanced fermionic density of states for 2D fermions.

IV. FINITE TRAPPING POTENTIAL AND CONCLUSIONS

We have shown that optical lattices strongly modify the behavior of Bose-Fermi mixtures via the appearance of van Hove singularities. The effect is most pronounced in two-dimensions, where the density of states diverges logarithmically, see Eq. (11). Then, for a fermionic chemical potential matching the position of the van Hove singularity, i.e., $\mu = \epsilon_0$, the mixture of bosons and fermions undergoes a second order phase transition at

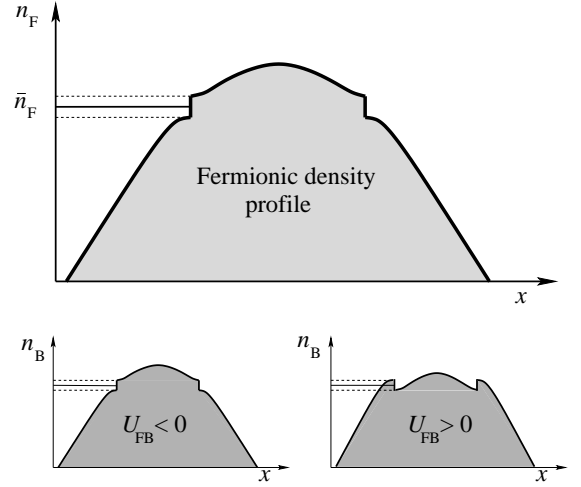


FIG. 2: Sketch of the fermionic and bosonic density profiles in the weak coupling limit $\lambda_{FB} \ll 1$. (a) The fermionic density exhibits a jump in the density by $2\delta\bar{n}_F$ as the first order transition line is crossed. At the same position in space, also the bosonic density exhibits a jump. For attractive interaction $U_{FB} < 0$ between the bosons and the fermions the bosonic density increases, see (b), while for repulsive interaction $U_{FB} > 0$ the bosonic density decreases at the jump (c).

the critical temperature T_{PS} . In analogy to the standard ‘liquid-gas’ gas transition, a fermionic density n_F with $\bar{n}_F - \delta\bar{n}_F < n_F < \bar{n}_F + \delta\bar{n}_F$ is unstable and inaccessible in an experiment for temperatures $T < T_{PS}$. The fermionic density profile in a harmonic trap can be derived from Eqs. (25) and (26), and its behavior at zero temperature and weak coupling is sketched in Fig. 2. The weak coupling $\lambda_{FB} \ll 1$ between the fermions and bosons makes sure that the density profile is only slightly modified compared to the noninteracting limit. As the local chemical potential $\mu(x)$ matches up with the van Hove singularity ϵ_0 , the fermionic density exhibits a jump by $2\delta\bar{n}_F$ related to the crossing of the first-order transition line. This behavior does not depend on the sign of the interaction U_{FB} between the bosons and fermions. In turn, the bosonic density profile strongly differs for attractive and repulsive U_{FB} . At the same position as the fermionic density profile exhibits a jump in the density, the bosonic density profile also exhibits a jump by $-2U_{FB}\delta\bar{n}_F/U_B$. The bosonic density increases similarly to the fermionic density profile for an attractive interaction $U_{FB} < 0$ between the bosons and fermions, while it is decreased for a repulsive interaction $U_{FB} > 0$, see Fig. 2. The different behavior of bosons and fermions is a consequence of the asymmetric role played by the constituents: the transition is driven by the van Hove singularity in the fermionic density of states and is independent on the bosonic density. Note that the situation is quite different in the strong coupling limit $\lambda_{FB} \approx 1$. Then the van Hove singularity in the density of states plays a minor role and the nature of the phase separated state is dominated by the character of

the interaction and the trapping potential, a situation previously discussed in Refs. 11, 12, 13, 14, 15, 16.

We have shown that the presence of van Hove singularities in the fermionic density of states produces new and interesting features in the context of phase separation in a 2D Bose-Fermi mixture. At the same time, these van Hove singularities also enhance the instabilities driving other quantum phases competing with phase separation. E.g., the instability towards BCS-superconductivity [17]

or the recent proposal for a supersolid phase [9] are both driven by Fermi-surface nesting, usually involving a $\ln(\epsilon_F/T)$ divergence which is enhanced to a $[\ln(\epsilon_F/T)]^2$ singularity in the presence of a van Hove singularity. 2D Bose-Fermi mixtures then are promising candidates for the observation of such new quantum phases, provided they successfully compete against the tendency towards phase separation lurking at T_{PS} .

-
- [1] A. G. Truscott, K. E. Strecker, W. I. McAlexander, G. B. Partridge, and R. G. Hulet, *Science* **291**, 2570 (2001).
 - [2] F. Schreck, L. Khaykovich, K. L. Corwin, G. Ferrari, T. Bourdel, J. Cubizolles, and C. Salomon, *Phys. Rev. Lett.* **87**, 080403 (2001).
 - [3] Z. Hadzibabic, C. A. Stan, K. Dieckmann, S. Gupta, M. W. Zwierlein, A. Görlitz, and W. Ketterle, *Phys. Rev. Lett.* **88**, 160401 (2002).
 - [4] G. Roati, F. Riboli, G. Modugno, and M. Inguscio, *Phys. Rev. Lett.* **89**, 150403 (2002).
 - [5] M. Houbiers, R. Ferwerda, and H. T. C. Stoof, *Phys. Rev. A* **56**, 4864 (1997).
 - [6] H. Heiselberg, C. J. Pethick, H. Smith, and L. Viverit, *Phys. Rev. Lett.* **85**, 2418 (2000).
 - [7] W. Hofstetter, J. I. Cirac, P. Zoller, E. Demler, and M. D. Lukin, *Phys. Rev. Lett.* **89**, 220407 (2002).
 - [8] L. Viverit, *Phys. Rev. A* **66**, 023605 (2002).
 - [9] H. P. Büchler and G. Blatter, *Phys. Rev. Lett.* **91**, 130404 (2003).
 - [10] M. Lewenstein, L. Santos, M. A. Baranov, and H. Fehrmann, *cond-mat/0307635* (2003).
 - [11] K. Mølmer, *Phys. Rev. Lett.* **80**, 1804 (1998).
 - [12] M. Amoroso, A. Minguzzi, S. Stringari, M. P. Tosi, and L. Vichi, *Eur. Phys. J. D* **4**, 261 (1998).
 - [13] N. Nygaard and K. Mølmer, *Phys. Rev. A* **59**, 2974 (1999).
 - [14] G. Modugno, G. Ferrari, G. Roati, R. J. Brecha, A. Simoni, and M. Inguscio, *Science* **297**, 1320 (2002).
 - [15] L. Viverit, C. J. Pethick, and H. Smith, *Phys. Rev. A* **61**, 053605 (2000).
 - [16] R. Roth and H. Feldmeier, *Phys. Rev. A* **65**, 021603 (2002).
 - [17] J. E. Hirsch and D. J. Scalapino, *Phys. Rev. Lett.* **56**, 2732 (1986).
 - [18] D. Jaksch, C. Bruder, J. I. Cirac, C. W. Gardiner, and P. Zoller, *Phys. Rev. Lett.* **81**, 3108 (1998).
 - [19] D. Y. Xing, M. Liu, and C. D. Gong, *Phys. Rev. B* **44**, 12525 (1991).
 - [20] M. Abramowitz and I. A. Stegun, *Handbook of Mathematical Functions* (Dover Publications, New York, 1972).
 - [21] H. P. Büchler, Ph.D. thesis, Swiss Federal Institute of Technology Zürich (2003).
 - [22] A. A. Abrikosov, L. P. Gorkov, and I. E. Dzyaloshinski, *Methods of Quantum Field Theory in Statistical Physics* (Dover Publications, 180 Varick Street, New-York 10014, 1963).